ISSN: 2472-3703 DOI: 10.6911/WSRJ.202605_12(5).0004

Research on Material Pile Volume Measurement Based on Laser 3D Measurement

Chuanming Zhang[1, *]

[1]School of Construction Machinery, Shandong Jiaotong University, Jinan, 250357, China

[*] Corresponding author

Abstract

A high-turnover stockpile storage system requires efficient and high-precision stock inventory capability. In this paper, a volume measurement method based on mean-drift clustering and density interpolation slicing method is proposed to solve the key technical problems such as multiple stockpile separation, point cloud sparsity and hole patching. For the point cloud data of material piles, the density interpolation slicing method is proposed, which detects low density and hole regions by selective frame interpolation, combines with the weighted average method to fill in the missing point cloud, and generates the closed outer contour by the improved contour scanning algorithm, and calculates the total volume layer by layer by accumulating using Shoelace's formula. The experimental results show that the selective frame interpolation method improves the accuracy by over 68% compared with the un-interpolated method, and the efficiency is better than that of 3D global interpolation under the condition of the same accuracy; the outer contour construction method in this paper improves the accuracy by over 80% compared with the traditional Graham algorithm, and the efficiency is better than that of Alpha Shape algorithm under the condition of the same accuracy. This method takes both accuracy and efficiency into account, and provides a reliable solution for the volume measurement of complex storage piles.

Keywords

Manuscripts; Calculation of material pile volume; Point cloud slicing; Slice selective interpolation; Sliced outer contour construction.

1. INTRODUCTION

In modern warehousing systems, accurately and efficiently measuring the volume of material piles, given their complex and varied shapes, has become crucial for optimizing inventory management, enhancing storage efficiency, and reducing costs[1]. With the advancement of warehousing automation and intelligence, traditional measurement methods, which involve manually piling materials into regular shapes and then calculating volume using geometric formulas, are increasingly inadequate for practical needs[2]. Therefore, addressing complex material pile morphologies and improving the accuracy and efficiency of volume measurement is becoming ever more important.

In the actual measurement of material pile volume, multi-view stereo measurement[3] and laser 3D measurement[4] are widely applied. Multi-view stereo measurement captures images of a material pile from multiple angles and uses computer vision techniques to reconstruct a 3D model for volume calculation[5]. Zhao Yingbao et al.[6] used a binocular camera to capture multiple sets of material pile images, employed an improved AD-Census algorithm for stereo

ISSN: 2472-3703 DOI: 10.6911/WSRJ.202605_12(5).0004

matching to generate 3D point cloud data of the pile, performed triangulation via Delaunay triangulation, and finally calculated the total pile volume by summing the volumes of geometric primitives, significantly reducing measurement error. Multi-view stereo measurement is suitable for scenarios with sufficient lighting and regularly shaped piles, but it may struggle to obtain accurate point cloud data when dealing with complex or highly irregular pile surfaces[7].

Laser 3D measurement acquires 3D coordinates of an object's surface via laser scanning. This method constructs a high-precision point cloud of the material pile by measuring the reflection time or phase difference of laser pulses combined with known emission directions, enabling non-contact measurement[8]. It has been applied in various fields including industry[9], construction[10], and agriculture[11]. Zeng Shufan et al.[12] proposed a laser measurement system combining servo motors and a laser rangefinder to build a 3D point cloud of powder piles inside storage silos, using an equal-unit cross-sectional area volume integration algorithm to estimate the powder volume. Experiments proved its accuracy to be better than 1%. The advantages of laser 3D measurement lie in its high precision, strong environmental adaptability, and wide measurement range, making it suitable for high-precision volume measurement in large-scale or complex environments[13]. However, in practical scanning, differences in material reflectivity and occlusion between piles can easily lead to point cloud sparsity and holes, causing distortion in 3D reconstruction and increasing volume measurement error. Furthermore, as single silos increasingly contain multiple coexisting piles, how to construct accurate and efficient pile extraction and volume calculation methods has become the core challenge for improving measurement accuracy and efficiency in dynamic warehousing environments[14].

Based on the above analysis, this paper adopts laser 3D measurement for material pile volume calculation. To address the issues of point cloud holes/sparsity in practical production, while balancing measurement accuracy and efficiency, the following improvements are proposed: a Density Interpolation Slicing Method is proposed. It grids the point cloud projection plane and calculates grid density to identify holes and sparse regions[15]. A weighted average interpolation method is used to complete the point cloud data in these regions. Combined with a convex hull scanning algorithm adapted to pile contours, it generates closed cross-sectional contours. The cross-sectional area is calculated using the Shoelace formula and summed to obtain the total volume, achieving a balance between accuracy and efficiency.

2. PROPERTIES

The slicing method [16] is a commonly used numerical technique for volume calculation. As shown in Figure 1, it involves segmenting a three-dimensional geometry into multiple thin layers along a specific direction. The point cloud of each layer is projected onto a common plane to form a two-dimensional contour. Subsequently, the area of each projected contour is calculated and multiplied by the height difference between adjacent slices to obtain the volume of the thin layer. Finally, the volumes of all layers are summed to derive the total volume.

In practical measurements, the traditional point cloud slicing method often introduces significant volume errors due to holes and sparsity in the point cloud, while 3D interpolation methods suffer from low efficiency when processing large-scale point cloud data. To address these challenges, a density-based interpolation slicing method is proposed. This method first performs selective interpolation on the 2D projection contour. The main principle involves identifying the extreme coordinates of the point cloud to determine an axis-aligned bounding box that encompasses all points. An appropriate grid cell size is then calculated using an empirical formula. Subsequently, the point cloud density within each grid cell is computed. Empty grid cells are discarded, and regions with densities below a set threshold are

ISSN: 2472-3703 DOI: 10.6911/WSRJ.202605_12(5).0004

interpolated and filled. This approach effectively mitigates issues related to sparsity and holes while improving algorithmic efficiency.

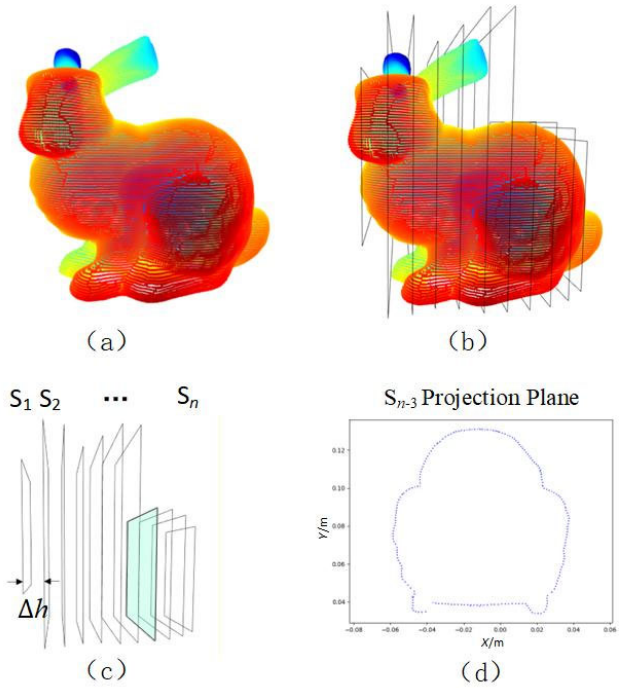

Figure 1. Schematic diagram of Volumetric Slicing Method. (a) 3D geometric point cloud model; (b) slice layer division; (c) layer extraction; (d) projection plane point cloud projection

Building on this, a convex hull scanning algorithm suitable for material pile point clouds is introduced. This algorithm selects the midpoint between the extreme points on the left and right boundaries of the projection as the starting reference point. Points are then connected sequentially based on their polar angles to generate a closed contour. This method is better suited to the multi-peak distribution characteristics of material pile point clouds, enhancing boundary recognition accuracy and further improving the precision of volume calculations. Finally, the area of the closed region is accurately computed using the Shoelace formula, achieving an efficient and precise volume measurement process.

2.1. Selective Frame Interpolation Method

The Selective Frame Interpolation Method is a local interpolation technique designed for sparse point clouds. By analyzing the local density of the point cloud projection grid, it identifies low-density regions and performs targeted interpolation. This approach effectively avoids the high computational cost associated with 3D global interpolation methods, thereby improving interpolation efficiency. Simultaneously, combined with weighted interpolation, it can fill hole regions and compensate for data loss in sparse areas, resulting in a more complete projection contour and enhancing the accuracy of volume measurement. The Selective Frame Interpolation Method consists of four main steps: slicing, grid generation and density calculation, threshold discrimination, and weighted interpolation and completion. The specific steps are as follows:

1)Divide grid and calculate point cloud density. As shown in Figure 2, the original point cloud is uniformly sliced along the z-axis direction. The point set for each thin layer $\{Q_i \mid z_i \le z \le z_i + h\}$ is extracted and projected onto the two-dimensional xy-plane. On the projection plane, the

ISSN: 2472-3703 DOI: 10.6911/WSRJ.202605_12(5).0004

minimum bounding box covering the point cloud range is established using $(x_{\min}, x_{\max})$ and $(y_{\min}, y_{\max})$. A buffer value δ is added in each direction to prevent point cloud data from being omitted when located at grid boundaries, Finally, an axis-aligned bounding box is formed to enclose the point cloud data and ensure the accuracy of subsequent calculations. Subsequently, the interior region of the bounding box is divided into a set of equally sized grids, where the grid resolution *l*must balance computational accuracy and computational efficiency. It can be determined using empirical formulas (Equation (1)). An appropriate grid scale can ensure smoothness while revealing data gaps in sparse regions.

$$l = \alpha \cdot \sqrt{\frac{A}{N}} \tag{1}$$

Here, A represents the area of the bounding box, N is the total number of points in the point cloud, and α is an empirical coefficient, typically chosen within the range $[0.5, 2]$. This selection ensures that each grid contains an appropriate number of points, avoiding excessive density or sparsity.

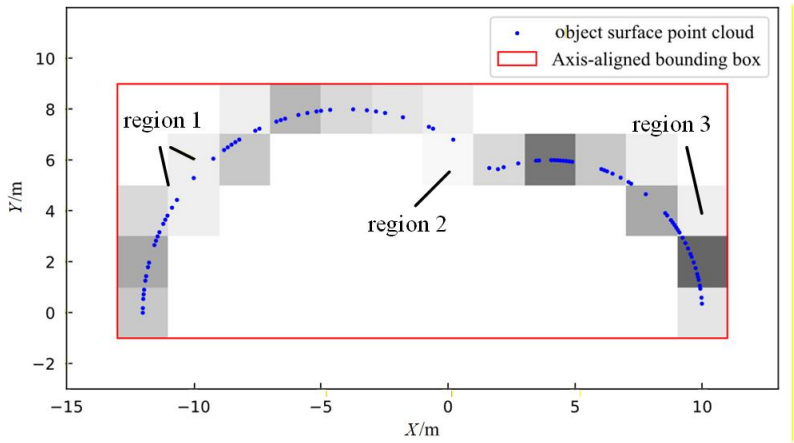

Figure 2. Grid partitioning of projected surface point cloud

Grids that do not contain any point cloud data are filtered out and discarded, retaining only the necessary grids. The number of points n_i and the point cloud density ρ_i within each remaining grid are calculated. The density ρ_i is defined as the ratio of the number of points in the grid to the area of the grid, as shown in Equation (2).

$$\rho_i = \frac{n_i}{l^2} \tag{2}$$

Based on the distribution characteristics of the point cloud and practical requirements, a density threshold ρ_{th} is set. If the density of a grid $\rho_i < \rho_{th}$, the point cloud in that region is considered sparse and requires interpolation for completion.

2)For regions within the grid where the point cloud density is below the threshold ρ_{th} (such as Region 1 in Figure 2) and for hole regions with evident data gaps (such as Region 2 in Figure 2), the weighted average interpolation method is employed to smooth the data. This method

ISSN: 2472-3703 DOI: 10.6911/WSRJ.202605_12(5).0004

performs interpolation using the weighted average of the k nearest neighbor points. Through reasonable weight assignment, the interpolation result reflects local characteristics while effectively compensating for data in sparse regions.

However, a significant density difference exists between sparse/hole regions and dense regions. Using a fixed number of points k for interpolation can easily lead to under-interpolation in sparse areas or over-interpolation in dense areas. To address this, a dynamic uniform sampling interpolation approach is proposed. Based on the density deficit $\Delta\rho = \rho_{\text{th}} - \rho_{ij}$ and the grid area l^2, the required number of interpolation points n_{in} is calculated as shown in Equation (3).

$$n_{\text{in}} = \left[\frac{\Delta\rho \cdot l^2}{d_{avg}} \right] \tag{3}$$

$$d_{\text{avg}} = \sqrt{l^2 / N_{\text{ref}}} \tag{4}$$

Here, d_{avg} denotes the average point spacing in high-density regions, defined by Equation (4), and N_{ref} is the average number of points in high-density grids. These values serve as references to ensure the interpolated density transitions naturally with the surrounding regions.

Subsequently, n_{in} uniformly distributed interpolation points $\{q_m\}$ are generated within the target grid. For each interpolation point $q = (x, y)$, its nearest neighboring points are $q_i = (x_i, y_i)$. The coordinate values (x, y) for the interpolated point, calculated via the weighted average method, are given by Equations (5) and (6) [18].

$$\hat{x} = \frac{\sum_{i=1}^{k} w_i x_i}{\sum_{i=1}^{k} w_i} \tag{5}$$

$$\hat{y} = \frac{\sum_{i=1}^{k} w_i y_i}{\sum_{i=1}^{k} w_i} \tag{6}$$

Here, w_i is the interpolation weight, which is typically related to the reciprocal of the distance, as defined in Equation (7) [18].

$$w_i = \frac{1}{d(q, q_i)} \tag{7}$$

In the equation, $d(q, q_i)$ represents the distance between the interpolation point q and its neighboring point q_i.

ISSN: 2472-3703 DOI: 10.6911/WSRJ.202605_12(5).0004

Dynamic uniform sampling interpolation adaptively adjusts the number of interpolation points driven by the density threshold. It increases density on demand in sparse regions while maintaining the original state in dense regions, thereby resolving the conflict between accuracy and efficiency. Additionally, as shown in Region 3 of Figure 2, the calculated density for point cloud data located at grid edges may fall below the set threshold ρ_{th}. Although such edge effect regions are typically also treated as sparse and subjected to interpolation, their impact on the overall interpolation result is relatively limited due to the smaller number of points at the edge positions.

2.2. Closed Contour Construction on the Projection Plane

After interpolation is completed, the point cloud data remains a set of discrete, unordered points lacking a base surface, making direct area calculation difficult. Therefore, it is necessary to first address the base surface problem, and then sort the boundary points and connect them sequentially to form a closed contour.

The Graham convex hull scanning algorithm selects the point with the minimum y (or x) coordinate in the point cloud as the initial point. Using this point as a reference, it sorts other points by polar angle and progressively eliminates concave points through cross-product judgment, thereby forming the minimum convex hull contour of the point cloud. However, for multi-peak material pile point clouds, as shown in Figure 3(b), boundary points in concave regions inevitably cause consecutive clockwise rotations (negative cross-product) and are thus considered "redundant points" by the algorithm. This rule can only generate a convex hull, losing the contour of the concave regions, and fails to meet the requirements for precise modeling. The Alpha Shape algorithm, based on Delaunay triangulation, captures the non-convex boundary characteristics of a point cloud by adjusting the boundary capture radius parameter α. It is suitable for precise boundary modeling of concave regions, but has high computational complexity when processing large-scale point clouds. Furthermore, in practical scanning scenarios, material pile point clouds often lack complete base surface data. The Alpha Shape algorithm may result in open (non-closed) boundaries, thereby affecting the accuracy of volume calculation.

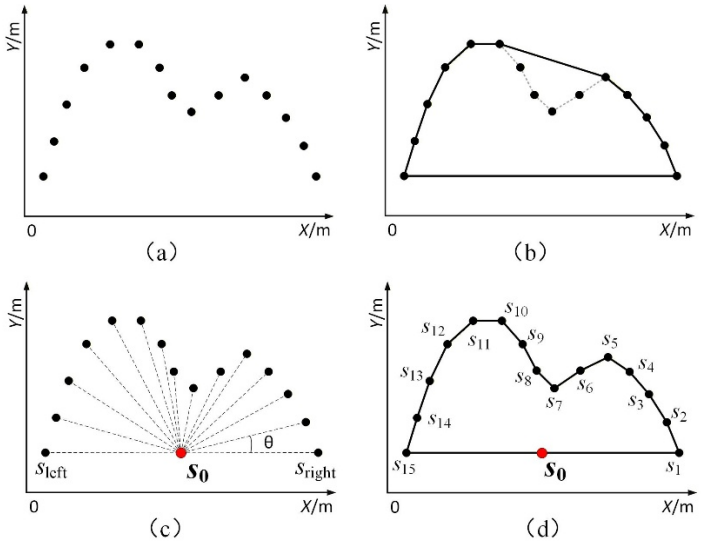

Figure 3. Illustration of point cloud cross-sectional contouring construction. (a)original point cloud data; (b)Graham scan algorithm; (c)polar angle sorting of point cloud; (d)contour construction completed

ISSN: 2472-3703 DOI: 10.6911/WSRJ.202605_12(5).0004

Aiming at the smooth and semi-closed characteristics of material pile surfaces, this paper proposes a convex hull scanning algorithm to construct a more precise outer contour for a given point cloud dataset S_a, as shown in Figure 3(a). As illustrated in Figure 3(c), the extreme points on the left and right sides of the two-dimensional projection boundary along the axis parallel to the ground, denoted as s_{left} and s_{right}, are selected. Their midpoint s_0 (calculated as per Equation (8)) is computed and added to the point cloud dataset S_a.

$$s_0 = \left(\frac{x_{left} + x_{right}}{2}, \frac{y_{left} + y_{right}}{2} \right) \tag{8}$$

This midpoint s_0 serves as the starting point, ensuring the adaptability of the initial point's position. The polar angles between all other points and s_0 are calculated as per Equation (9). Sorting these points in ascending order of their polar angles yields the ordered point cloud dataset S_b. Starting from s_0, each point in S_b is traversed sequentially. As shown in Figure 3(d), after sequential connection, a closed, ordered convex hull boundary point set $S_c = \{s_0, s_1, s_2 \ldots, s_k\}$ is obtained.

$$\theta_i = arctan\left(\frac{y_i - y_0}{x_i - x_0} \right) \tag{9}$$

As can be seen from Figure 3, when s_0 is set as the initial point, connecting it to the two extreme points on either side effectively forms the base contour of the material pile. This leverages the horizontal distribution characteristic of the pile's bottom boundary, thereby solving the point cloud semi-closure problem. Selecting the midpoint of the extreme points optimizes the starting point's position, bringing it closer to the geometric center of the material pile point cloud. This helps suppress false hull errors between dual peaks, resulting in a more regular and geometrically sound outer contour for the point cloud.

In summary, the proposed outer contour construction method utilizes the horizontal linear distribution property of point clouds at the pile's base. Through the geometrically centralized starting mechanism and the multi-peak contour capture rule, it overcomes the rigid convex hull constraint inherent in the traditional Graham algorithm, which relies on cross-product direction judgment. This enables precise capture of boundary points in concave regions. Compared to the Alpha Shape algorithm, it avoids complex global 3D computations, significantly improving computational efficiency. Consequently, it achieves a unification of high efficiency and high fidelity in volume measurement for complex material piles.

2.3. Material Volume Calculation

After obtaining the polygon on the projection plane in Section 1.2, the area of the closed shape is calculated using the Shoelace formula [16] (see Equation (10)). The Shoelace formula essentially sums the alternating products of the coordinates of the polygon's boundary points. It decomposes the complex geometric area calculation into simple algebraic operations, eliminating the need for further triangulation and thereby improving both efficiency and accuracy. For the boundary point set S_c, let the convex hull vertices be sequentially denoted as (x_i, y_i).

ISSN: 2472-3703 DOI: 10.6911/WSRJ.202605_12(5).0004

$$A=\frac{1}{2}\left|\sum_{i=1}^{k-1}\left(x_i y_{i+1}-y_i x_{i+1}\right)+\left(x_k y_1-y_k x_1\right)\right| \tag{10}$$

For each slice, the volume of a layer is considered as a column approximately parallel to the projection plane. Therefore, by multiplying the cross-sectional area with the slice thickness h, the volume of that individual slice is obtained. Subsequently, the volumes of all slices are summed to yield the total volume of the material pile, as shown in Equation (11).

$$V=\sum_{i=1}^{n}A_i\cdot\left(z_{i+1}-z_i\right)=\sum_{i=1}^{n}A_i\cdot\Delta h \tag{11}$$

Here, A_i is the cross-sectional area of the i-th slice.

3. TESTS

This experiment utilized a RoboSense Helios 16 lidar paired with a Haitai HS-S-6025 brushless motor gimbal to collect point cloud data of the material pile's outer contour. The lidar and gimbal were transported to a position above the material pile by an inspection robot and a rail system. A real-time connection to a computer was established via a wireless network bridge, enabling the transmission of the collected point cloud data for processing. The scanning hardware system is illustrated in Figure 4.

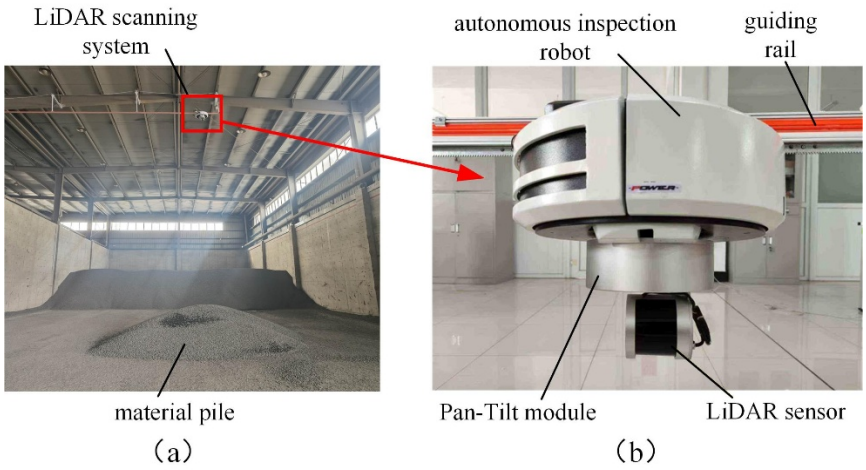

Figure 4. 3D Scanning hardware system. (a) Volumetric scanning platform; (b) LiDAR scanning system

The hardware environment for processing the material pile point cloud data was as follows: an Intel i5-9300H processor, an NVIDIA GeForce GTX 1660Ti graphics card, and 16GB of RAM. A photograph of the actual material pile is shown in Figure 5(a). The point cloud data of the material pile, collected and preprocessed within the Open3D library in the Visual Studio Code environment, is shown in Figure 5(b).

ISSN: 2472-3703 DOI: 10.6911/WSRJ.202605_12(5).0004

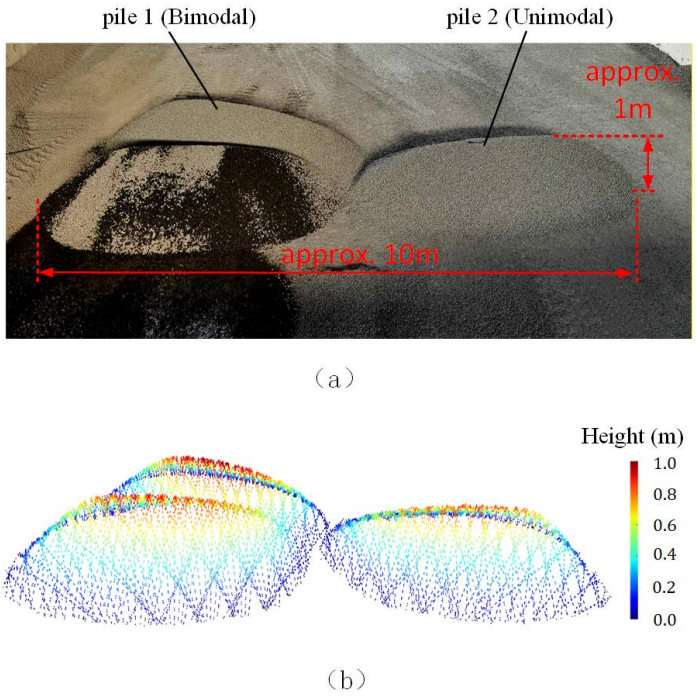

Figure 5. Material pile scanning results. (a) Scanned material pile samples;(b) Material pile point cloud data

3.1. Local Interpolation Using the Selective Frame Interpolation Method

To validate the advantages of the Selective Frame Interpolation Method in terms of volume calculation accuracy and efficiency, experiments were conducted to measure the volume of a material pile using three different point cloud processing approaches: the no-interpolation method, the 3D global interpolation method, and the Selective Frame Interpolation Method. The segmented bimodal pile 1 shown in Figure 5 was selected as the subject of the study.

In the experiments, the point cloud data of the actual material pile was processed using the three aforementioned methods for volume calculation. The results were compared against the actual volume. Evaluation metrics included volume error and runtime. The experimental measurement results are shown in Table 2, a comparison of calculation accuracy is presented in Figure 6, and the efficiency comparison between 3D global interpolation and the Selective Frame Interpolation Method under the same accuracy level is shown in Table 1.

The experimental results indicate that the no-interpolation method exhibited significant volume errors, reaching 9.08% especially at a slice thickness of 0.1m. This demonstrates that accurate volume calculation is difficult without applying interpolation to the pile's point cloud. The 3D global interpolation method achieved the best accuracy, but with longer runtime and higher complexity, its efficiency was significantly lower than that of the Selective Frame Interpolation Method. Compared to the no-interpolation method, the Selective Frame Interpolation Method controlled the volume error within 3%, representing an accuracy improvement greater than 68%. Furthermore, it demonstrated superior efficiency to the 3D global interpolation method at the same accuracy level and maintained comparable accuracy as the slice thickness was gradually reduced.

ISSN: 2472-3703 DOI: 10.6911/WSRJ.202605_12(5).0004

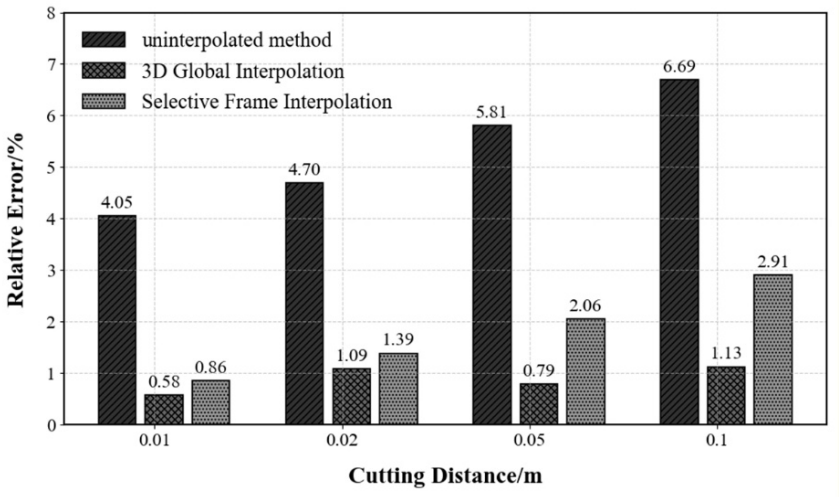

Figure 6. Volume calculation accuracy comparison of three interpolation methods

Table 1. Comparative analysis of volumetric computation efficiency between two interpolation methods

Interpolation method	Precision≥98%		Precision≥99%	
	Cutting Distance/m	Time/s	Cutting Distance/m	Time/s
3D Global Interpolation	0.2	34.82	0.08	39.138
Selective Frame Interpolation	0.04	7.047	0.01	17.941
Improvement	—	**79.76%**	—	**54.16%**

Table 2. Performance comparison of three interpolation methods

Actual Volume /m³	Cutting Distance/m	Uninterpolated method			3D Global Interpolation			Selective Frame Interpolation		
		Volume/ m³	Relative Error/%	Time /s	Volume /m³	Relative Error/%	Time/ s	Volume /m³	Relative Error/%	Time/s
4.316	0.01	4.491	4.05	0.444	4.341	0.58	42.369	4.353	0.86	17.941
	0.02	4.519	4.7	0.483	4.363	1.09	41.643	4.376	1.39	9.356
	0.05	4.567	5.81	0.258	4.282	0.79	39.7	4.226	2.06	4.391
	0.1	4.605	6.69	0.219	4.365	1.13	38.825	4.442	2.91	2.565

3.2. Closed Outer Contour Construction

Based on the point cloud data completed by the Selective Frame Interpolation Method described in Section 1.1, three algorithms were employed for outer contour construction and subsequent volume calculation: the Graham convex hull scanning algorithm, the Alpha Shape algorithm, and the scanning algorithm proposed in this paper. Since the Alpha Shape algorithm requires a closed point cloud model as input, its input data was supplemented with base surface point clouds in the experiment to generate a closed surface. By comparing the volume relative error (%) and runtime (s) of the three algorithms, the comprehensive advantages of the proposed algorithm in terms of both accuracy and efficiency were validated. Table 4 and Figure 7 present the volume calculation accuracy of the three outer contour construction methods, while Table 3 shows the efficiency comparison between the proposed algorithm and the Alpha Shape algorithm under the same accuracy requirement.

The experimental results indicate that the Graham convex hull scanning algorithm, due to its inability to recognize the geometric features of concave regions in the material pile, leads to lower accuracy in the generated outer contour for complex-shaped (bimodal) piles, resulting in overestimated volume measurements (with a relative error reaching 15.22% at a slice thickness

ISSN: 2472-3703 DOI: 10.6911/WSRJ.202605_12(5).0004

of 0.1m). Although the Alpha Shape algorithm achieves higher accuracy, its runtime is significantly longer compared to the proposed algorithm. In contrast, while the volume calculation accuracy of the proposed scanning algorithm is slightly lower than that of the Alpha Shape algorithm at the same slice thickness, its runtime is substantially reduced under the same accuracy requirement, demonstrating an efficiency improvement of approximately 70%.

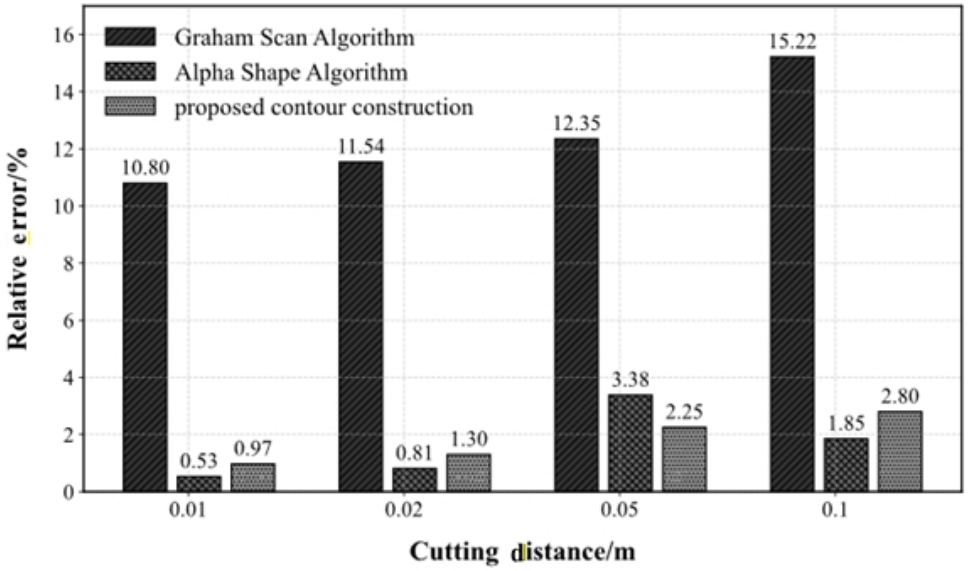

Figure 7. Volumetric computation accuracy of three contour construction algorithms

Table 3. Comparative efficiency of two contour construction algorithms in volumetric computation

Scanning algorithm	Precision≥98%		Precision≥99%	
	Cutting Distance/m	Time/s	Cutting Distance/m	Time/s
Alpha Shape Algorithm	0.12	30.581	0.04	61.872
Proposed contour construction	0.04	7.317	0.01	18.109
Improvement	—	**76.1%**	—	**70.73%**

Table 4. Comparative measurement results of three contour construction methods

Actual volume/ m^3	Cutting Distance/m	Graham Scan Algorithm			Alpha Shape Algorithm			Proposed scanning algorithm		
		Volume/ m^3	Relative Error/%	Time/s	Volume /m^3	Relative Error/%	Time/s	Volume /m^3	Relative Error/%	Time/s
4.316	0.01	4.782	10.8	18.541	4.293	0.53	157.902	4.358	0.97	18.109
	0.02	4.814	11.54	10.903	4.351	0.81	88.1	4.372	1.3	9.057
	0.05	4.849	12.35	5.771	4.462	3.38	56.323	4.219	2.25	4.355
	0.1	4.973	15.22	3.108	4.396	1.85	36.394	4.437	2.8	2.996

3.3. Experiments and Analysis of the Density Interpolation Slicing Method

The advantages of the Selective Frame Interpolation Method and the proposed outer contour scanning method within the Density Interpolation Slicing Method were established in Sections 2.1 and 2.2. This section compares the complete Density Interpolation Slicing Method with the traditional method (3D global interpolation + Alpha Shape algorithm). A comparison of volume relative errors is shown in Figure 8, and a comparison of runtime is presented in Figure 9.

Analyzing the volume calculation results, the algorithm's accuracy is inversely proportional to the initial slice thickness. Under the same slice thickness, the volume calculation accuracy of the Density Interpolation Slicing Method is slightly lower than that of the traditional method.

ISSN: 2472-3703 DOI: 10.6911/WSRJ.202605_12(5).0004

However, in terms of efficiency, its overall runtime is superior to the traditional slicing method. This advantage is particularly significant at smaller slice thicknesses (e.g., 0.01m), where the computation time for the traditional method increased to 178.531s, while the Selective Frame Interpolation Method required only 18.109s, demonstrating a marked efficiency improvement.

Table 5 further quantifies the efficiency gain of the two methods. Under the condition of an accuracy requirement greater than 98%, the computation time for the Alpha Shape algorithm was 46.119s, whereas the proposed scanning algorithm required only 7.355s, representing an efficiency improvement of 85.82%. When the accuracy requirement was increased to 99%, the proposed method still maintained a computational efficiency advantage of 70.73% over the traditional method. These results prove that the proposed method achieves a significant improvement in computational efficiency while ensuring high accuracy.

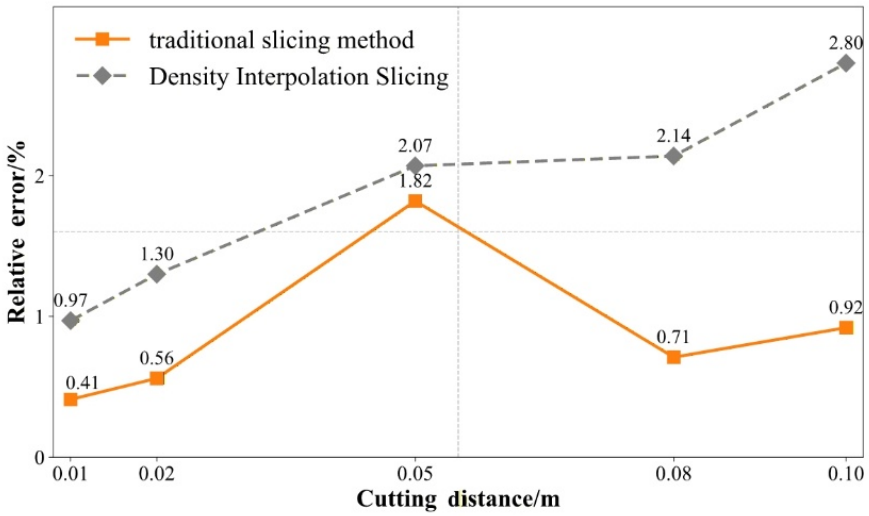

Figure 8. Computational time analysis between Density Interpolated Slicing and traditional slicing method

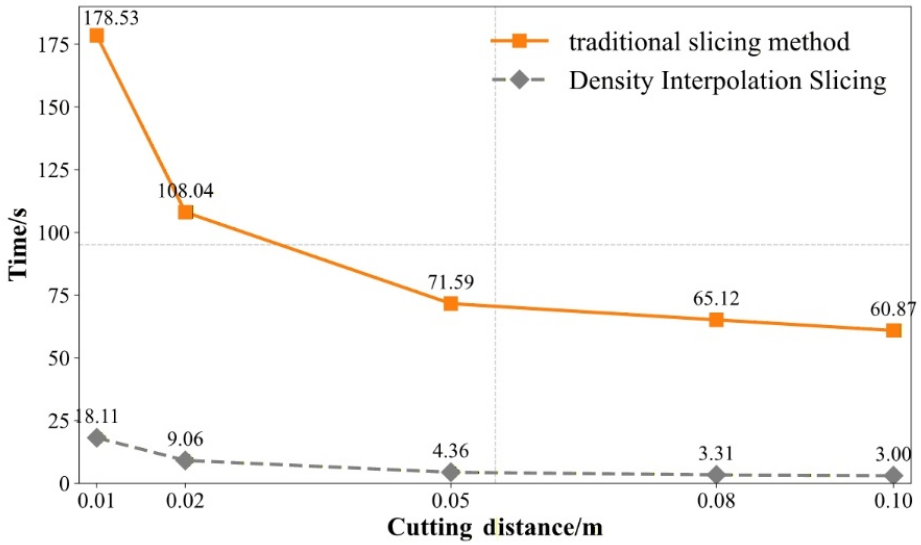

Figure 9. Computational time comparison between Density Interpolation and traditional slicing method

ISSN: 2472-3703 DOI: 10.6911/WSRJ.202605_12(5).0004

Table 5. Comparative efficiency analysis between Density Interpolation Slicing and traditional slicing method in volumetric computation

Volume calculation method	Precision≥98%		Precision≥99%	
	Cutting Distance/m	Time/s	Cutting Distance/m	Time/s
Traditional method	0.19	46.119	0.1	69.869
Density Interpolation Slicing	0.04	7.355	0.01	18.109
Improvement	—	**84.05%**	—	**70.73%**

4. CONCLUSION

In the volume calculation stage, this paper proposes a Density Interpolation Slicing Method, which incorporates two main improvements over traditional slicing methods. First, to address point cloud sparsity and holes, a Selective Frame Interpolation Method is proposed. By analyzing the local density of the point cloud projection grid, it identifies low-density regions at the two-dimensional level and performs selective weighted average interpolation. This significantly improves interpolation efficiency while maintaining accuracy, substantially reducing computational costs compared to 3D global interpolation methods. Second, a method for constructing closed outer contours on the projection plane, suitable for material pile morphology, is proposed. This method selects the extreme points on either side of the axis parallel to the ground on the projection plane, uses their midpoint as the starting point, sorts the remaining points by polar angle, and connects them sequentially to generate a closed contour, thereby enhancing the adaptability of contour construction. Experimental results demonstrate that the Density Interpolation Slicing Method significantly improves computational efficiency compared to traditional methods while ensuring high accuracy, providing an efficient and stable technical solution for volume measurement of material piles in complex environments.

The method presented in this paper balances both accuracy and efficiency, solving key technical problems such as hole completion. However, certain limitations remain: the Selective Frame Interpolation Method relies on 2D projection planes for interpolation, which may lead to accuracy loss in regions with drastic morphological changes. Future research could focus on constructing a dynamic mapping model between the bandwidth parameter and local point cloud density, automatically adjusting the kernel function's scope of action through density gradient awareness, or introducing 3D local feature information into the 2D projection plane of the Selective Frame Interpolation Method to improve the algorithm's adaptability and the accuracy of volume calculation.

REFERENCES

[1] Wu B Y,Wang S J, Lin H J, et al. Fast Estimation of Loader's Shovel Load Volume by 3D Reconstruction of Material Piles[J]. Chinese Journal of Mechanical Engineering. 2023, 36(5): 202-220.

[2] Li F, Wei W X, Sun X, et al. Method for Volume Measurement and Calculation of Asphalt Aggregate Based on UAV Technology[J]. Journal of Beijing University of Technology, 2022, 48(6): 580-588.

[3] LIU G X, XIAO T G，CHEN G Y, et al. An in-situ volume measurement method for storage tanks based on MVSNet multi-view stereo deep learning[J]. China Measurement, 2023, 49(01): 26-30.

[4] Michael L, Melissa M .Volume estimates of trees with complex architecture from terrestrial laser scanning[J].Journal of Applied Remote Sensing, 2008, 2(01): 023521-1-023521-19.

ISSN: 2472-3703 DOI: 10.6911/WSRJ.202605_12(5).0004

[5] ZHEN S, LIN Y S, SHENG Y F, et al. Measurement of sea cucumber volume using binocular vision[J]. Transactions of the Chinese Society of Agricultural Engineering (Transactions of the CSAE), 2024, 40(21): 165-174.

[6] ZHAO Y B, LI H W, HUANG L M, et al. Material Pile Volume Measurement Based on Binocular Stereo Vision and Point Cloud Registration[J], Metal Mine, 2025, (03): 138-147.

[7] LEI G.The Research of Material pile Volume measurement Based on Multi-vision[D]. Shenyang: Northeastern University, 2012.

[8] Cihan A .Review of Scanning and Pixel Array-Based LiDAR Point-Cloud Measurement Techniques to Capture 3D Shape or Motion[J]. Applied Sciences, 2023, 13(11): 6488.

[9] Juliastuti E, Nadhira V, Zahra N, et al.Laser Distance Meter for Cylinder Tank Volume Measurement System[J].In Fourth International Seminar on Photonics, Optics, and Its Applications (ISPHOA 2020), 2021, 11789.

[10] LI A R, DENG W B, HOU X Q.Application of 3D Laser Scanning Technology in Ancient Building Surveying and Mapping[J]. Geospatial Information, 2022, 20(07): 101-103.

[11] Cai Z, Jin C, Xu J, et al. Measurement of Potato Volume With Laser Triangulation and Three-Dimensional Reconstruction[J]. IEEE Access 8 (2020): 176565-176574.

[12] ZHEN F S, HE H W,FU K P, et al. Study on the residual volume measurement system of laser scanning[J]. China Measurement, 2022, 48(12): 74-79.

[13] Nguyen T A, Nguyen P T, and Do S T.Application of BIM and 3D laser scanning for quantity management in construction projects[J]. Advances in Civil Engineering 2020.1 (2020): 8839923.

[14] WEN L Y, PANG K. Adaptive mean shift clustering based on cover-tree[J]. Computer Engineering and Design, 2024, 45(02): 452-458.

[15] MA X L.Research on Key Technologies of Sheep 3D Reconstruction Based on 3D Point Cloud[D]. Neimenggu: Inner Mongolia Agricultural University, 2023.

[16] Meng X L, Wang T Y, Cheng D Y, et al.Enhanced Point Cloud Slicing Method for Volume Calculation of Large Irregular Bodies: Validation in Open-Pit Mining[J]. Remote Sensing, 2023, 15(20): 5006.